Hindawi Publishing Corporation
EURASIP Journal on Wireless Communications and Networking
Volume 2008, Article ID 735410, 11 pages
doi:10.1155/2008/735410

Research Article

Combining OOK with PSM Modulation for Simple Transceiver of Orthogonal Pulse-Based TH-UWB Systems

Sudhan Majhi,[1] A. S. Madhukumar,[1] A. B. Premkumar,[1] and Paul Richardson[2]

[1] *School of Computer Engineering, Nanyang Technological University, Block-N4, Nanyang Avenue, Singapore 639798*
[2] *Electrical and Computer Engineering, University of Michigan, Dearborn, MI 48128, USA*

Correspondence should be addressed to Sudhan Majhi, sudh0001@ntu.edu.sg

Received 21 November 2007; Revised 2 June 2008; Accepted 22 July 2008

Recommended by Weidong Xiang

This paper describes a combined modulation scheme for time-hopping ultra-wideband (TH-UWB) radio systems by using on-off keying (OOK) and pulse-shape modulation (PSM). A set of orthogonal pulses is used to represent bits in a symbol. These orthogonal pulses are transmitted simultaneously in the same pulse repetition interval resulting in a composite pulse. This scheme transmits the same number of bits by using fewer orthogonal pulses and receiver correlators than those used in PSM and biorthogonal PSM (BPSM). The proposed scheme reduces multiple-access interference and multipulse interference considerably by using crosscorrelation properties of orthogonal pulses. Since each bit is individually received by OOK, the proposed scheme requires less power. Hence, it is applicable for energy constrained and low-cost TH-UWB systems. The bit-error-rate (BER) performance is analyzed both mathematically and through computer simulations under the different channel environments. The performance of this scheme is compared with that of existing PSM and its combined modulation schemes by using two sets of orthogonal pulses.

1. INTRODUCTION

The successful deployment of ultra-wideband (UWB) radio systems for high-speed indoor communication strongly depends on the development of pulses, modulation techniques, and low-complexity receivers. For time-hopping ultra-wideband (TH-UWB) systems, symbols are transmitted using short-analog waveforms confined to the power and spectrum range specified for UWB radios [1]. Various kinds of modulation schemes such as pulse-position modulation (PPM), orthogonal PPM (OPPM), pulse-amplitude modulation (PAM), on-off keying (OOK), and biphase modulation (BPM) have been proposed for TH-UWB radio to achieve better system performance and high data rate transmission [2, 3]. However, due to increased intersymbol interference (ISI) in the presence of multipath channel, M-ary PPM or M-ary orthogonal PPM (OPPM) for TH-UWB systems may not be an effective modulation scheme for higher values of M [4, 5]. M-ary PAM also has limited applications for any short-range and low-power communication systems [6]. Although the OOK scheme is easy-to-implement, it cannot be used for higher-level modulation schemes for high data rates due to its binary nature.

Due to its robustness against ISI and multiple-access interference (MAI), PSM is an interesting research topic in TH-UWB, direct sequence UWB (DS-UWB), and transmitted reference UWB (TR-UWB) radio systems [7–10]. However, due to speculative autocorrelation property of higher-order orthogonal pulses, PSM cannot be used for higher-level modulation schemes for improving system data rate. Moreover, it requires a large number of receiver correlators and system complexity increases nonlinearly with increasing M.

To address these problems, combined with PSM schemes such as biorthogonal PSM (BPSM), BPSK-PSM, and 2PPM-PSM have been proposed to transmit the same amount of data using fewer orthogonal pulses and receiver correlators [11–14]. However, biorthogonal PSM requires $M/2$ orthogonal pulses and receiver correlators. BPSK-PSM scheme is a polarity-dependent modulation scheme. Designing an antipodal signal for orthogonal pulses is more difficult compared to nonantipodal signal [15]. 2PPM-PSM requires coded modulation to maintain orthogonality of constellation vectors and needs external memory in the receiver to improve system performance. OPPM-BPSM is a combined modulation scheme that was proposed for high data rates

[16]. However, this scheme does not reduce the number of receiver correlators, resulting in high system complexity. Moreover, most of these combined schemes have been analyzed in AWGN environment and have not been considered in multipath channel environments [12, 13].

To deal with these challenges, a combined modulation scheme based on OOK and PSM for M-ary modulation schemes was proposed to reduce system complexity by using OOK for higher-level modulation schemes [14]. This preliminary work was based on an AWGN channel, and interference reduction was seen only in MAI. In this paper, multipath environments are considered by using two different sets of orthogonal pulses. Due to multipath and pulse orthogonality, two interference terms, interpulse interference (IPI) and multipulse interference (MPI), are considered in place of ISI. The cross-correlation properties of the orthogonal pulses reduce MPI, improving the system performance in multipath scenarios when compared to single-pulse systems. The present paper discusses the details of transceiver structure for an OOK-PSM system, its performance, and a detailed interference modeling under multipath scenarios. To compare it with existing schemes, PSM and its combined modulation schemes are also analyzed using a multipath channel [4].

This paper is organized as follows. Section 2 describes OOK-PSM modulation scheme and its advantages. Section 3 discusses transmission and detection procedures with the assumed correlator receiver structure. Section 4 shows interference issues and system performance of OOK-PSM scheme using RAKE reception. Section 5 discusses the simulation results under different channel environments in the presence of multiple users.

2. PROPOSED COMBINED MODULATION SCHEME

The proposed method maps a set of message bits or symbol onto one or several orthogonal pulses by on-off keying. The number of pulses in each symbol depends on the number of non-zero bits in the symbol. Table 1 shows examples of 2-bit and 3-bit symbol transmissions and the corresponding transmitted pulses. In general, N-bit symbol requires N orthogonal pulses to transmit OOK-PSM signals. These N independent bits are sent at the same time by assigning different orthogonal pulses resulting in a composite pulse. The presence of individual orthogonal pulses in the composite pulse is decided by on-off keying, (i.e., pulse is present for *one* and is absent for *zero*). Since pulses are orthogonal, they overlay in both time and frequency domains without any interference [17].

The composite pulse passes through a set of correlators in the receiver. The receiver correlators are designed using a set of template signals which are similar to the set of orthogonal pulses used in the transmitter. Each correlator recovers a pulse from the composite pulses by exploiting its correlation properties. The composite pulses for 3-bit symbols are shown in Figure 1.

The proposed method has several advantages over conventional methods. For example, it uses fewer orthogonal pulses and receiver correlators than those used in PSM and

Table 1: Transmitted pulses for 2-bit and 3-bit symbols.

Schemes		T_f			Combined form of transmitted pulses
		$w_0(t)$	$w_1(t)$	$w_2(t)$	
2-bit	00	Off	Off	Off	None
	01	Off	Off	On	$w_2(t)$
	10	Off	On	Off	$w_1(t)$
	11	Off	On	On	$w_1(t) + w_2(t)$
3-bit	000	Off	Off	Off	None
	001	Off	Off	On	$w_2(t)$
	010	Off	On	Off	$w_1(t)$
	011	Off	On	On	$w_1(t) + w_2(t)$
	100	On	Off	Off	$w_0(t)$
	101	On	Off	On	$w_0(t) + w_2(t)$
	110	On	On	Off	$w_0(t) + w_1(t)$
	111	On	On	On	$w_0(t)+w_1(t)+w_2(t)$

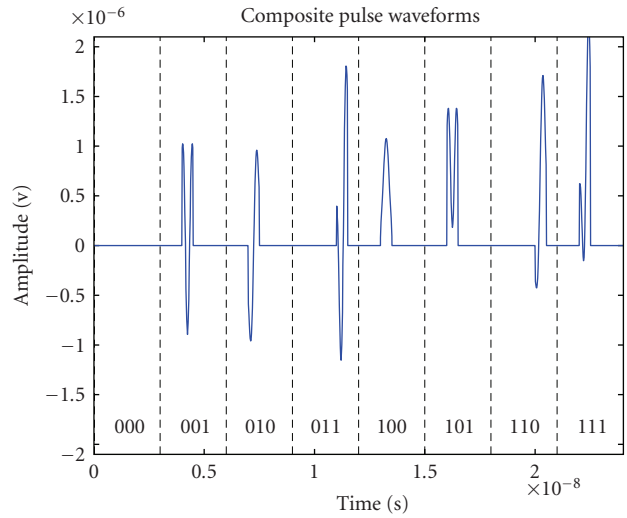

Figure 1: Composite MHPs for a 3-bit OOK-PSM modulation scheme.

biorthogonal PSM schemes. This leads to lower complexity for system design. Since *zero* is represented by absence of pulse, the proposed scheme uses low average transmit power, which is critical for energy-constrained UWB communication systems. Further, complexity of OOK is nearly half of that of other conventional modulation schemes and is easier-to-implement. This complexity reduction and simplicity are applicable when OOK is combined with other modulation schemes.

Since the proposed scheme uses orthogonal pulses, MAI can be reduced considerably by assigning different subsets of orthogonal pulses for different users. MPI is also reduced by using cross-correlation properties of orthogonal pulses. Moreover, it transmits more bits using fewer orthogonal pulses, it generates fewer spectral spikes in the signal [12]. Therefore, the proposed scheme can coexist with overlapping narrowband systems without causing significant interference [18]. The overall scheme is downward compatible. That is

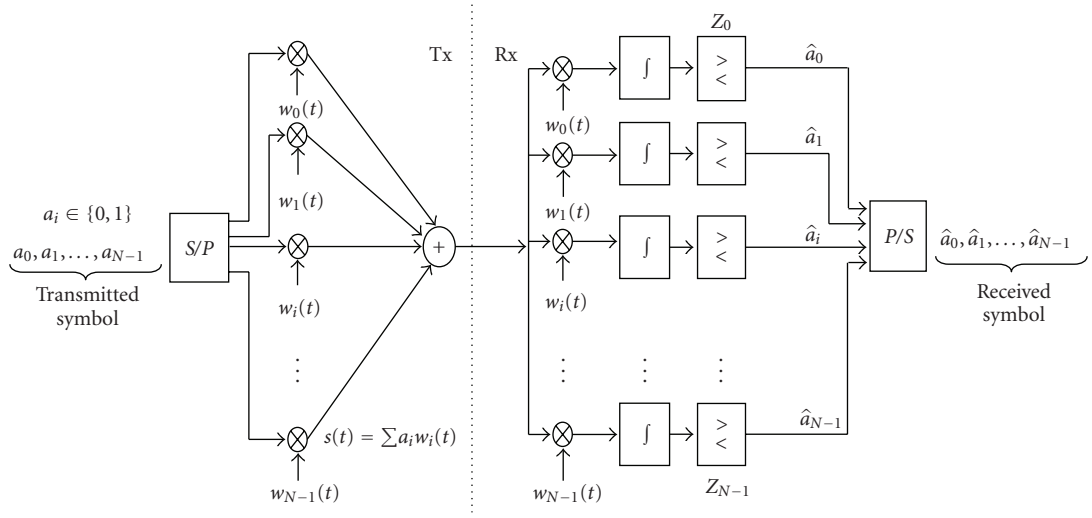

Figure 2: Correlation transceiver structure for N-bit OOK-PSM modulation scheme in AWGN channel.

and hence the higher-level modulation schemes can be used for lower level modulation systems without changing the hardware design. For example, 3-bit scheme can be changed into 2-bit scheme by just keeping off $w_0(t)$ or changed into binary scheme by keeping off $w_0(t)$ and $w_1(t)$. This property can be exploited further for adaptive modulation systems based on channel conditions at any given instant.

For multiple-access systems, design of transmitted signal depends on the modulation scheme and TH-codes to avoid catastrophic collision among users. The OOK-PSM modulation signal of the kth user for the ith symbol can be defined as

$$s_i^{(k)}(t) = \sqrt{E_{tx}^{(k)}} \sum_{j=0}^{N_s-1} \mathbf{a}_i \mathbf{w}^{(\mathbf{k})}\left(t - jT_f - c_j^{(k)} T_c\right), \tag{1}$$

where $i = 0, 1, \ldots, M-1$, N_s is the number of pulse repetition interval for a symbol, $E_{tx}^{(k)}$ is the transmitted energy of kth user, T_f is the pulse repetition interval, index j represents the number of pulse repetition intervals for a symbol, $c_j^{(k)}$ is the TH sequence with chip duration T_c, and

$$\mathbf{w}^{(k)}(t) = \left[w_0^{(k)}(t) w_1^{(k)}(t) \cdots w_{N-1}^{(k)}(t)\right]^T \tag{2}$$

is the N-dimensional column vector of kth user, $w_n^{(k)}(t)$ is the nth-order orthogonal pulse of kth user, and $\mathbf{a_i}$ is the N-bit binary row data vector for the ith symbol.

3. PERFORMANCE OF OOK-PSM IN AWGN CHANNEL

The system performance and receiver structure depend on modulation schemes and channel models. In this section, system performance is analyzed with the assumed correlator receiver structure. Correlator-based transceiver structure for N-bit OOK-PSM modulation scheme is shown in Figure 2. The correlator receiver contains N correlators for N-bit OOK-PSM scheme. Since the system supports N_u users, the received signal in additive white Gaussian noise (AWGN) channel is written as

$$r(t) = \sum_{k=1}^{N_u} \sqrt{E_{rx}^{(k)}} s^{(k)}\left(t - \tau^{(k)}\right) + n(t), \tag{3}$$

where $\tau^{(k)}$ is the time delay for kth user, $E_{tx}^{(k)}$ is the received energy of kth user, and $n(t)$ is the AWGN, assumed to have a two-sided power spectral density of $N_0/2$. The received signal passes through N correlators. In each correlator, the received signal is multiplied by template signal and the corresponding transmission bit is decided by exploiting correlation properties of the orthogonal pulses. Hard decision decoding is assumed at the correlator to detect a bit, followed by a parallel-to-serial converter to detect a symbol. However, the receiver performance can be improved by using high-performance soft-decision decoding method.

The number of correlators in the receiver is the same as the number of bits in a symbol. If N_s is the number of repetition interval for a symbol, the reference bit b is defined in the time interval $[0, T_b]$, where $T_b = N_s T_f$. The decision statistic of user 1 is

$$\begin{aligned} y &= \int_0^{T_b} r(t) \mathbf{w}^{(1)}\left(t - jT_f - c_j^{(1)} T_c\right) dt \\ &= \sum_{k=1}^{N_u} \int_0^{T_b} \left(\sqrt{E_{rx}^{(k)}} s^{(k)}\left(t - \tau^{(k)}\right) + n(t)\right) \mathbf{w}^{(1)}\left(t - jT_f - c_j^{(1)} T_c\right) dt \\ &= \left[Z_0 \;\; Z_1 \;\; \cdots \;\; Z_{N-1}\right]^T, \end{aligned} \tag{4}$$

where $\mathbf{w}^{(1)}(t)$ is the template signals defined in (2), neglecting transceiver derivative characteristics and Z_l is the test statistic of lth correlator which undergoes a hard decision decoding, where $l = 0, 1, \ldots, N-1$. The value of Z_l can be expressed as

$$Z_l = Z_{l,s} + Z_{l,\mathrm{MAI}} + Z_{l,n}, \tag{5}$$

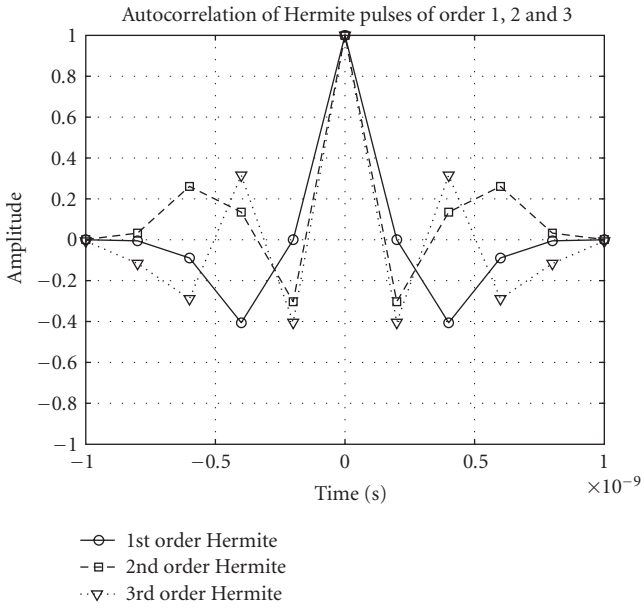

Figure 3: Autocorrelation values of short duration MHPs of 1st-, 2nd-, and 3rd-order pulses.

where $Z_{l,s}$ is the desired signal, $Z_{l,\mathrm{MAI}}$ is the MAI term, and $Z_{l,n}$ is the AWGN term at the lth correlator. Each of these terms are explained in the following paragraphs.

Assuming perfect synchronization, desired signal $Z_{l,s}$ can be expressed as

$$Z_{l,s} = \sum_{j=0}^{N_s-1} \int_{jT_f+c_j^{(1)}T_c}^{jT_f+c_j^{(1)}T_c+T_c} \sqrt{E_{rx}^{(1)}}\, s^{(1)}(t) w_l\left(t - jT_f - c_j^{(1)}T_c\right) dt, \tag{6}$$

where $w_l(t)$ is the template signal of lth correlator. The useful pulse of the desired user takes place within the chip duration T_c, so the time frame $[jT_f, (j+1)T_f]$ changes into $[jT_f + c_j^{(1)}T_c, jT_f + c_j^{(1)}T_c + T_c]$. Assuming that an lth-order pulse is present in the composite pulse, the signal energy of the user 1 at the lth correlator for N_s time frame is obtained by

$$E_b^{(1)} = \left(Z_{l,s}\right)^2 = E_{rx}^{(1)} N_s^2 \int_0^{T_c} h_l^2(t)dt = E_{rx}^{(1)} N_s^2, \tag{7}$$

where $E_{rx}^{(k)}$ is the received amplitude of the kth user.

Under standard Gaussian approximation, $Z_{l,n}$ and $Z_{l,\mathrm{MAI}}$ are assumed to be zero-mean Gaussian random processes as characterized by variances σ_n^2 and σ_{MAI}^2, respectively. Due to timing jitter (ϵ) error from $N_u - 1$ interfering users, ϵ is uniformly distributed over $[\Delta, -\Delta]$, where $\Delta = 0.1$ nanosecond for modified Hermite pulses (MHPs) up to 4th order [7, 19, 20]. The total MAI at lth correlator $Z_{l,\mathrm{MAI}}$ can be expressed as [21]

$$Z_{l,\mathrm{MAI}} = \sum_{k=2}^{N_u} \sum_{j=0}^{N_s-1} \int_{jT_f}^{(j+1)T_f} s^{(k)}\left(t - \tau^{(k)} - \epsilon\right) w_l\left(t - jT_f - c_j^{(1)}T_c\right) dt. \tag{8}$$

As the timing jitter error from interfering user is very small when compared to $\tau^{(k)} \in [0, N_sT_f]$, one can assume that $\tau^{(k)} + \epsilon \approx \tau$ is uniformly distributed over the interval $[0, N_sT_f]$. Therefore, the total interference energy from other users can be evaluated as

$$\sigma_{l,\mathrm{MAI}}^2 = \frac{N_s}{T_f} \sum_{k=2}^{N_u} \int_0^{T_f} \left(\sqrt{E_{rx}^{(k)}} \int_0^{T_p} w_n^{(k)}(t-\tau) w_l(t) dt\right)^2 d\tau, \tag{9}$$

where T_p is the width of pulses, $w_n^{(k)}$ is the nth-order pulses from the kth user. If all users use the same set of orthogonal pulses, n takes any value from the set $\{0, 1, \ldots, N-1\}$ and if all users use different exclusive orthogonal subsets, n is not equal to l, where l is the order of pulse waveform of user 1 and is used at the lth correlator. It can be assumed that $E_{rx}^{(1)} = E_{rx}^{(2)} = \cdots = E_{rx}^{(N_u)} = E_{rx}$ for perfect power control for all users. Since correlation value depends on the width of the pulses, (9) can be expressed as

$$\begin{aligned} \sigma_{l,\mathrm{MAI}}^2 &= \frac{N_s}{T_f} E_{rx} \sum_{k=2}^{N_u} \int_0^{T_p} \left(\int_0^{T_p} w_n^{(k)}(t-\tau) w_l(t) dt\right)^2 d\tau \\ &= \frac{N_s}{T_f} E_{rx} \sum_{k=2}^{N_u} \int_0^{T_M} \left(R_{n,l}^{(k)}(\tau)\right)^2 d\tau, \end{aligned} \tag{10}$$

where $R_{n,l}^{(k)}(\tau)$ is the correlation between nth and lth-order pulses. The term $R_{n,l}^{(k)}(\tau)$ becomes $R_{l,l}^{(k)}(\tau)$ or $R_l^{(k)}(\tau)$ if the kth user uses lth-order pulses in the given time $[0, N_sT_f]$. Due to correlation properties of orthogonal pulses, the term $R_{n,l}^{(k)}$ is always lesser than $R_{l,l}^{(k)}(\tau)$ for the synchronized system. In conventional systems, the above correlation term is always between the same pulses and is referred to as autocorrelation value and the sum of these autocorrelation values gives significant amount of MAI; but for orthogonal pulse-based modulation schemes, MAI is considerably less due to the low cross-correlation values added with autocorrelation values. The MAI can be reduced further by sharing mutually exclusive orthogonal subsets among the different users. In this case, MAI contains only cross-correlation values. The autocorrelation and cross-correlation values of MHPs are shown in Figures 3 and 4, respectively.

However, $Z_{l,n}$ is the AWGN at the lth correlator output:

$$Z_{l,n} = \sum_{j=0}^{N_s-1} \int_{jT_f}^{(j+1)T_f} n(t) w_l\left(t - jT_f - c_j^{(1)}T_c\right) dt, \tag{11}$$

and the corresponding variance, that is, noise power of AWGN can be expressed as follows [13]:

$$\sigma_n^2 = \frac{N_sN_0}{2} \int_0^{T_f} w_l^2(x)dx = \frac{N_sN_0}{2}. \tag{12}$$

The probability of symbol error rate can be written as from Appendix A:

$$P_r = \left(1 - \prod_{l=0}^{N-1} \left(1 - Q\left(\sqrt{\mathrm{SNR}}\right)\right)\right). \tag{13}$$

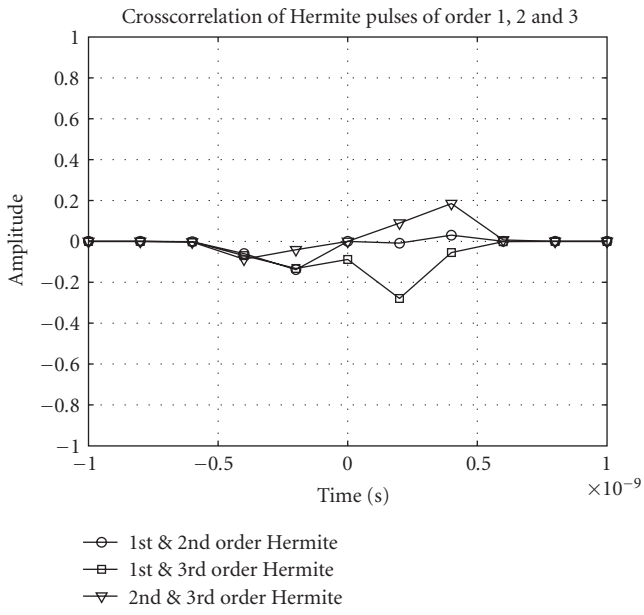

Figure 4: Crosscorrelation values of short duration MHPs of 1st-, 2nd-, and 3rd-order pulses.

4. PERFORMANCE IN MULTIPATH CHANNEL

The system performance of the orthogonal pulse-based modulation scheme decreases in the presence of multipath channel. The RAKE fingers are used to collect the strongest multiple components of a signal. Figure 5 shows the RAKE receiver structure for multipath channel model. The complexity of RAKE receiver scheme increases with the number of strong multipath components. The performance and robustness of a system in multipath environment is often determined by the amount of multipath energy that can be collected at the receiver. If there are N_u users and each experiences a different channel model, then the received signal can be expressed as

$$r(t) = \sum_{k=1}^{N_u} \sum_{l=1}^{L_p} \alpha_l^{(k)} s^{(k)}\left(t - \tau_l^{(k)}\right) + n(t), \tag{14}$$

where $\alpha_l^{(k)}$ is the path gain and $\tau_l^{(k)}$ is the time delay of lth path for kth user, and $n(t)$ is the AWGN. The reference signal of user 1 at qth $(= 0, 1, \ldots, N-1)$ correlator can be expressed as

$$\phi_q^{(1)}(t) = \sum_{j=0}^{N_s-1} v_q^{(1)}\left(t - jT_f - c_j^{(1)} T_c\right), \tag{15}$$

where N_s is the total number of time frame for a symbol and

$$v_q^{(1)}(t) = \sum_{p=1}^{L_p} \alpha_p^{(1)} w_q^{(1)}\left(t - \tau_p^{(1)}\right). \tag{16}$$

Since multiple pulses are transmitted in single-time frame, the transmitted signal contain several pulses. However, template signal at each RAKE finger in the receiver

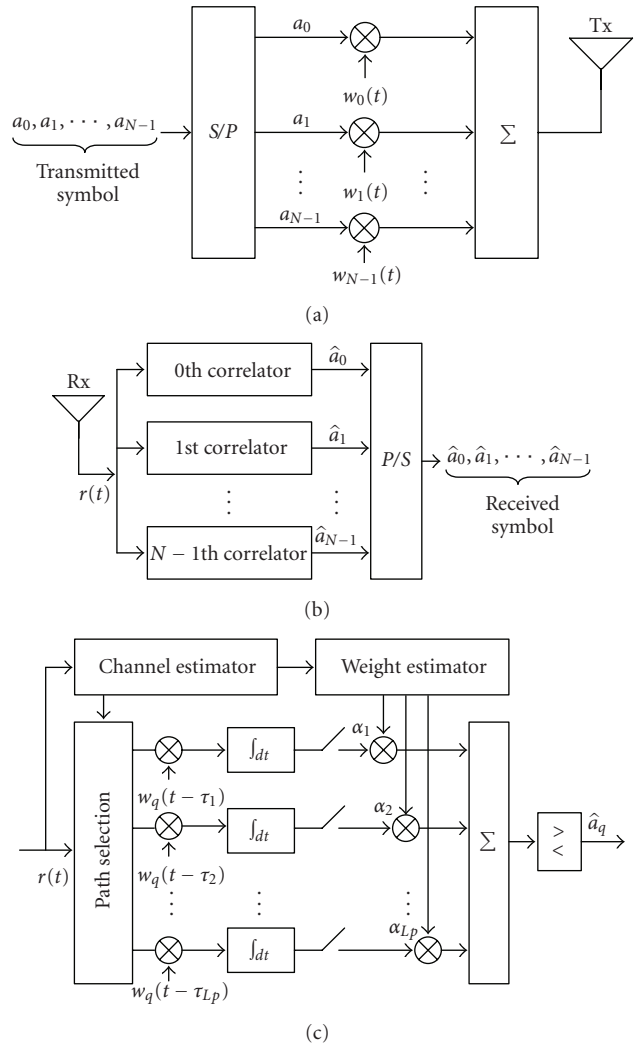

Figure 5: (a) A simple transmitter structure for N-bit OOK-PSM scheme. (b) Receiver structure for combined N-bit OOK-PSM scheme. (c) RAKE receiver structure for qth $(q = 0, 1, \ldots, N-1)$ correlator.

contains only one pulse. That is, the sum of several pulses is correlated with single pulse waveform, which creates interferences in the presence of timing jitter and in asynchronous systems. The pulses with short duration are not orthogonal and they may overlap with one another. When a pulse overlaps with itself, it is called interpulse interference (IPI) or self-interference and when pulse interferes with other pulses, it is called multipulse interference (MPI). The decision statistics of user 1 in the qth correlator can be written as

$$\begin{aligned} Z_q^{(1)} &= \int_{jT_f}^{(j+1)T_f} r(t)\phi_q^{(1)}(t)dt \\ &= S_q^{(1)} + \mathrm{IPI}_q^{(1)} + \mathrm{MPI}_q^{(1)} + \mathrm{MAI}_q^{(1)} + N_q^{(1)}, \end{aligned} \tag{17}$$

where $S_q^{(1)}$ is the desired signal, $\mathrm{IPI}_q^{(1)}$ is the IPI, $\mathrm{MPI}_q^{(1)}$ is the MPI, $\mathrm{MAI}_q^{(1)}$ is the MAI due to presence of multiple users, and $N_q^{(1)}$ is the AWGN term. The IPI, MPI, MAI, and

AWGN terms behave like an interference noise mixed with the original signal. The correct decision of $Z_q^{(1)}$ is possible only if the desired signals, IPI, MPI, MAI, and AWGN are known precisely. Therefore, these terms need to be analyzed.

4.1. Desired signal

For analysis, it is assumed that perfect synchronization exists between transmitter and the reference receiver. Assuming that $\tau_l^{(1)} = 0$ and the transmitted symbol uses qth-order pulse, $w_q^{(1)}(t)$, the desired average signal $S_q^{(1)}$, can be expressed as [22, 23]

$$\begin{aligned} S_q^{(1)} &= \sqrt{E_{tr}^{(1)}} \sum_{j=0}^{N_s-1} \sum_{p=1}^{L_p} \alpha_p^{(1)} \alpha_p^{(1)} \\ &\quad \times \int_0^{T_f} w_q^{(1)}\left(t - c_j^{(1)} T_c - \tau_p^{(1)}\right) w_q^{(1)}\left(t - c_j^{(1)} T_c - \tau_p^{(1)}\right) dt \\ &= \sqrt{E_{tr}^{(1)}} N_s \sum_{p=1}^{L_p} \left(\alpha_p^{(1)}\right)^2. \end{aligned} \tag{18}$$

It is observed that the received energy in multipath channel increases with the increase in the number of RAKE fingers. This improves system performance at the cost of system complexity. Therefore, a tradeoff between performance and system complexity is required to design a reliable system for multipath channel.

4.2. Interpulse interference (IPI)

IPI is related to interference with the same-order pulses and depends on the number of multipath components in the signal but is not concerned with the number of users in the system. The average variance of $\mathrm{IPI}_q^{(1)}$ can be written from Appendix B as

$$\sigma_{\mathrm{IPI}}^2 = E_{tr}^{(1)} N_s T_f^{-1} \sum_{p=1}^{L_p} \sum_{l=1}^{L_p} \sum_{\substack{p'=1 \\ p' \neq p}}^{L_p} \sum_{\substack{l'=1 \\ l' \neq l}}^{L_p} \alpha_p^{(1)} \alpha_l^{(1)} \alpha_{p'}^{(1)} \alpha_{l'}^{(1)} X(\Delta), \tag{19}$$

where $X(\Delta) = E\{R_{qq}^{(1,1)}(\tau_l^{(1)} - \tau_p^{(1)}) R_{qq}^{(1,1)}(\tau_{l'}^{(1)} - \tau_{p'}^{(1)})\}$. The IPI degrades the system performance when systems are not synchronized and improves for synchronized with orthogonal pulses. Designing orthogonal pulses with short duration is an important and challenging task for OOK-PSM modulation scheme.

4.3. Multipulse interference (MPI)

MPI is related to interference with different-order pulses and depends on the number of multipath components. It does not depend on the number of users in the system. The average variance of $\mathrm{MPI}_q^{(1)}$ can be written from Appendix B

$$\sigma_{\mathrm{MPI}}^2 = E_{tr}^{(1)} N_s T_f^{-1} \sum_{p=1}^{L_p} \sum_{l=1}^{L_p} \sum_{\substack{p'=1 \\ p' \neq p}}^{L_p} \sum_{\substack{l'=1 \\ l' \neq l}}^{L_p} \sum_{\substack{m=1 \\ m \neq q}}^{N} \sum_{\substack{m'=1 \\ m' \neq q'}}^{N} \alpha_p^{(1)} \alpha_l^{(1)} \alpha_{p'}^{(1)} \alpha_{l'}^{(1)} Y(\Delta), \tag{20}$$

MPI also degrades the system performance for higher cross-correlation values of orthogonal pulses in both synchronized and a synchronized systems. Since $Y(\cdot)$ is the expectation of product of $R_{qm}^{(1,1)}(\cdot)$ and $R_{q'm'}^{(1,1)}(\cdot)$, $R_{qm}^{(1,1)}(\cdot)$ is the cross-correlation value of two different-order pulses q and m which tends to zero. MPI tends to be zero for perfect orthogonal pulses and synchronized systems irrespective of the number of multipaths are present in the received signal.

4.4. Multiple-access interference

Under ideal conditions, the receiver is not affected by the presence of multiple transmissions for perfectly orthogonal TH-codes. In practice, however, systems do not achieve ideal synchronization and codes lose orthogonality due to different propagation delays from different paths. The receiver might not be able to remove undesired signals completely and as a consequence, system performance is affected by MAI [2, 21, 24]. The average variance of $\mathrm{MAI}_q^{(1)}$ can be written from Appendix B as

$$\begin{aligned} &\sigma_{\mathrm{MAI}}^2 \\ &= N_s T_f^{-1} \sum_{k=2}^{N_u} \sum_{k'=2}^{N_u} \sqrt{E_{tr}^{(k)}} \sqrt{E_{tr}^{(k')}} \sum_{p=1}^{L_p} \sum_{l=1}^{L_p} \sum_{p'=1}^{L_p} \sum_{l'=1}^{L_p} \alpha_p^{(1)} \alpha_l^{(k)} \alpha_{p'}^{(1)} \alpha_{l'}^{(k)} V(\Delta'), \end{aligned} \tag{21}$$

where $V(\Delta') = E\{R_{qq'}^{(1,k)}(\Delta_1) R_{qq'}^{(1,k)}(\Delta_2)\}$ and $\Delta_2 = (c_j^{(1)} - c_j^{(k')}) T_c - (\tau_{p'}^{(1)} - \tau_{l'}^{(k')})$. In a single-user system, MAI is zero and in a multiple-user system MAI is zero if TH-codes are orthogonal and users are synchronized irrespective of the pulse characteristic. However, designing synchronized systems and using orthogonal TH-codes is a difficult task for TH-UWB transceiver. Therefore, MAI can be reduced by using orthogonal-based modulation schemes and assigning different exclusive orthogonal subsets for different users.

4.5. Bit-error rates

Due to the different autocorrelation values for different pulses, each correlator gives a different probability of error. It can easily be proved that the noise/interference terms are zero-mean Gaussian variables, and so the corresponding probability of error of the lth correlator in the presence of IPI, MPI, and MAI can be written as [20]

$$P_l = Q\left(\sqrt{\frac{\left(S_q^{(1)}\right)^2}{2\left(\sigma_{\mathrm{IPI}}^2 + \sigma_{\mathrm{MPI}}^2 + \sigma_{\mathrm{MAI}}^2 + \sigma_N^2\right)}}\right), \tag{22}$$

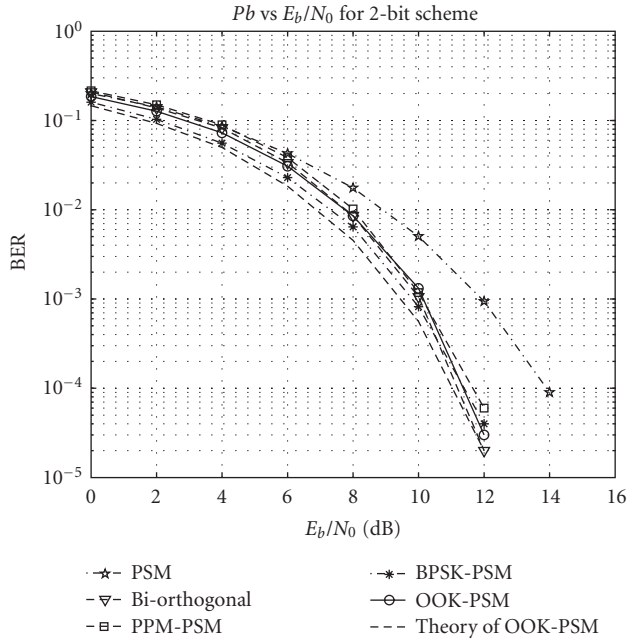

Figure 6: Performance of PSM, BPSM, PPM-PSM, BPSK-PSM, and OOK-PSM for 2-bit symbols transmission scheme for modified Hermite pulses in AWGN.

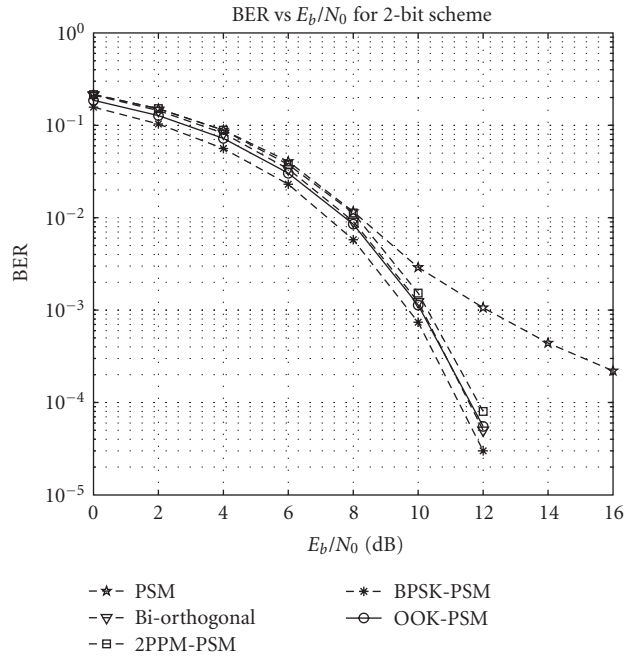

Figure 7: Performance of PSM, BPSM, PPM-PSM, BPSK-PSM, and OOK-PSM for 2-bit symbols transmission scheme for PSWF pulses in AWGN.

where σ_N^2 is defined in Appendix B. Since each decision is independent, the average probability of bit errors and symbol errors can be obtained in similar way shown in Appendix A.

5. SIMULATION RESULTS AND DISCUSSION

In this section, simulation results for 2-bit PSM and its combined schemes are analyzed. The simulation studies are conducted in AWGN and IEEE802.15.3a UWB multipath channel under the assumption of perfect synchronization. The present simulation studies assume a fixed-threshold level. Since threshold value is insensitive to number of users, a fixed-threshold value $\theta_{\text{th}} = \gamma\sqrt{E_{tx}}$ has been chosen rather than selecting optimum threshold values adaptively, where γ is normalized threshold value. For multipath channel, a standard method based on [25] is used to obtain γ. The present simulation studies use $\gamma = 0.5$ for AWGN channel and $\gamma = 0.75$ for CM1 channel. All simulations studies use MHPs and prolate spheroidal wave functions (PSWFs) orthogonal pulses without using any coding or guard interval [7, 11, 12].

5.1. AWGN component

The performance of 2-bit OOK-PSM scheme in AWGN channel using MHPs and PSWFs is shown in Figures 6 and 7, respectively. It can be seen that all combined modulation schemes out perform PSM scheme. Due to fewer pulses and receiver correlators than those used in PSM, the proposed scheme provides low complexity for system design. It does not require a large number of orthogonal pulses and receiver correlators for higher-level modulation schemes. Since it uses few orthogonal pulses for transmission, it creates fewer spectral spikes resulting in better coexistence with overlapping NB systems.

When compared with BPSM scheme, the proposed scheme requires fewer pulses and receiver correlators for similar data rates. For a 2-bit modulation scheme, OOK-PSM shows nearly the same performance as that of BPSM. Due to limited correlation properties of higher-order orthogonal pulses, the proposed scheme performs better than BPSM-based system when the number of bits per symbol is increased.

From Figures 6 and 7, it can be observed that BPSK-PSM results in slightly better performance than that in OOK-PSM scheme. Since the performance difference between conventional BPSK and OOK is 3 dB in AWGN channel, it is also expected that performance of BPSK-PSM should give 3 dB over OOK-PSM scheme. As the number of bits per symbol increases, the performance difference between BPSK-PSM and OOK-PSM decreases. This is because of the increased average number of pulses in the BPSK-PSM modulation when compared with OOK-PSM. For example, in 2-bit BPSK-PSM scheme, each symbol requires two orthogonal pulses, whereas OOK-PSM requires one pulse except for symbol 11 which requires two pulses. This difference in number of average pulses is more visible when the number of bits per symbol is increased. Though the pulses are said to be orthogonal, they are not orthogonal in the finite time interval, as shown in Figures 3 and 4 [7]. This leads to degradation in the performance of BPSK-PSM when the number of average pulses is more within the same time interval.

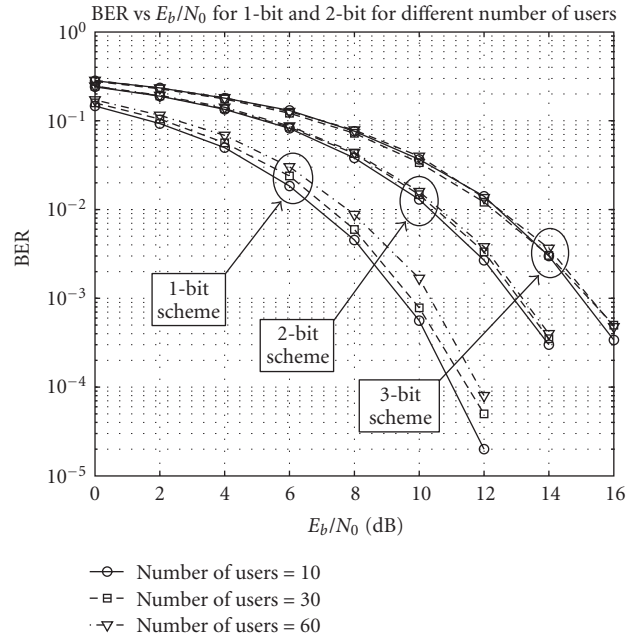

Figure 8: Performance of 1-bit, 2-bit, and 3-bit symbols transmission of the OOK-PSM scheme for different numbers of users in AWGN.

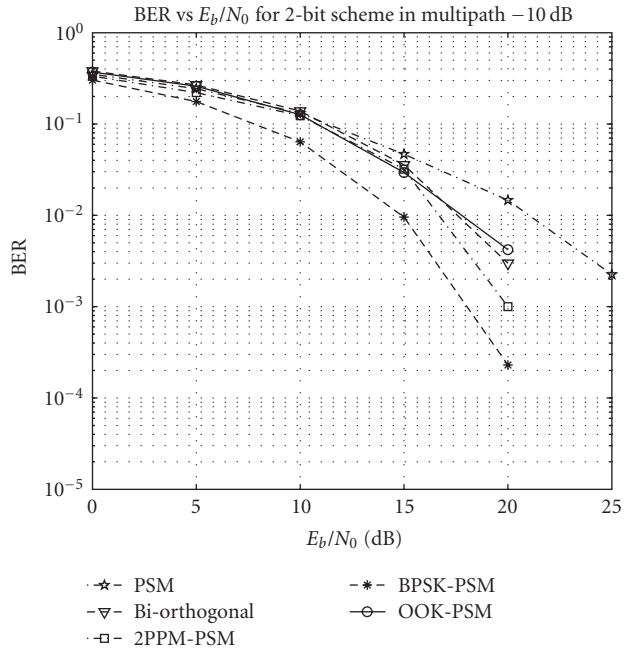

Figure 9: Performance of various modulation schemes for 2-bit symbols transmission in a multipath environments. The receiver assumes a RAKE-combination by considering all paths within −10 dB of the strongest path. The schemes uses orthogonal pulses based on MHPs.

It can be seen that the proposed scheme results in nearly the same performance as that of 2PPM-PSM scheme. However, due to presence of nonorthogonal pulse position in 2PPM-PSM scheme, ISI and MAI issues resurface in 2PPM-PSM modulation scheme which can severely affect system performance in multipath environments. Maintaining orthogonality of the constellation vector is important for better system performance. So, it requires coded modulation and memory in the receiver to achieve the orthogonality of constellation vector [12, 26]. Since 2PPM-PSM scheme uses pulse positions, amplitudes, and orthogonal pulses, recovering of signals at the receiver is complicated in the presence of multipath. In addition, the complexity of system design for 2PPM-PSM is increased by the presence of constellation matrix, map-decision vector, and distance-comparator vector in the receiver [27].

In Figure 8, the performance in multiple user environment is presented in AWGN channel. It can be seen that performance decreases with increase in the number of bits per symbol. This is largely because of the increase in the number of orthogonal pulses used for signal transmission. Since pulses are not strictly orthogonal within the finite interval, interference among these pulses leads to performance degradation. However, across multiple users, the performance degradation is minimal. On the other hand, due to presence of a single pulse in 1-bit transmission, the performance difference with respect to users is more visible; but in 2-bit and 3-bit schemes, performance difference with respect to number of users is less visible. This is because these schemes use multiple orthogonal pulses which reduce cross-correlation terms in MAI in synchronized systems. The simulation results justify the lower MAI compared to single-pulse systems as shown in (10).

5.2. Multipath channel model

Since orthogonal pulses are sensitive to multipath channel, it is required to analyze the performance of PSM modulation and its combined scheme in the presence of multipath. Channel estimation is done by using selective RAKE receiver and maximum ratio combining (MRC). The number of significant paths is decided by taking all paths within 10 dB of the strongest path. To collect all these multipaths, a RAKE-combining method is employed at the receiver. It is assumed that the transmitted pulse average interval is much longer than the pulse duration. In channel estimation, only distinguishable paths are selected.

Figures 9 and 10 show the performance of combined PSM schemes by using MHPs and PSWFs, respectively, where the number of RAKE fingers is 17. The PSWFs give better performance than MHPs in the presence of multipath. From the figures, it can be seen that the proposed OOK-PSM shows better performance than the PSM scheme, but BPSK-PSM gives better performance than all the other modulation schemes. Since zero is represented by pulse off, OOK complexity is nearly half of that in any other modulation scheme. Therefore, M-ary OOK-PSM compensates lesser system performance with lower complexity design. Although other modulation schemes give nearly the same performance, due to simplicity of OOK scheme, its combined form with PSM is an appropriate choice for system design with low cost.

6. CONCLUSION

This paper discusses a combined modulation scheme for N-bit symbol transmission by using fewer orthogonal pulses

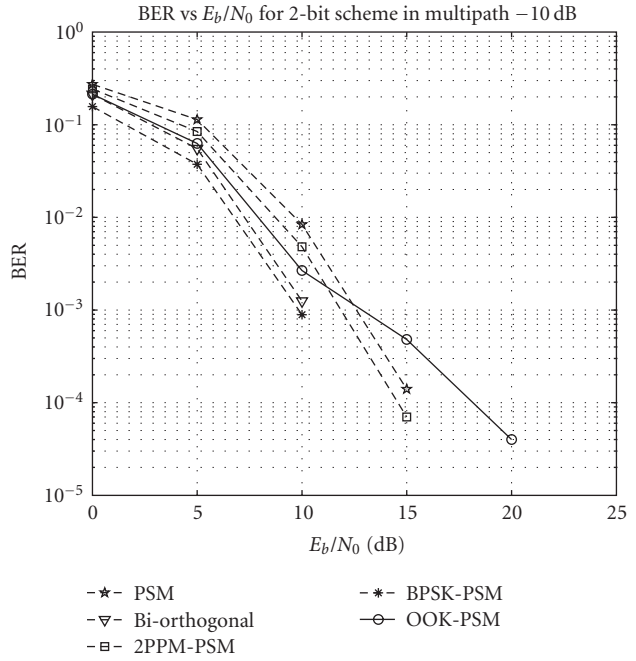

Figure 10: Performance of various modulation schemes for 2-bit symbols transmission in a multipath environments. The receiver assumes a RAKE-combination by considering all paths within −10 dB of the strongest path. The schemes uses orthogonal pulses based on PSWFs.

and receiver correlators than those used in conventional PSM and biorthogonal PSM schemes. Using OOK modulation, the proposed scheme reduces system complexity and needs minimum average transmitted power, which is critical for low-cost and energy-constrained UWB systems. The orthogonal pulses reduce MAI in the presence of multiple users, and give better system performance in AWGN environment than conventional single-pulse systems. This paper also shows the performance of PSM and its combined schemes in multipath channel model. The proposed scheme can be used for low-complexity, energy-constrained, and multiple-access UWB communication systems without degrading the data rate of existing combined schemes.

APPENDICES

A. AWGN ENVIRONMENTS

Due to different autocorrelation values for different orders of pulses, each correlator gives different probability of error. By using (7), (10), and (12), probability of error of the lth correlator in the presence of MAI can be written as

$$P_l = Q\left(\sqrt{\frac{E_b^{(1)}}{2\left(\sigma_n^2+\sigma_{l,\mathrm{Mai}}^2\right)}}\right) = Q\left(\sqrt{\frac{N_s^2 E_{rx}}{2\left(\sigma_n^2+\sigma_{l,\mathrm{Mai}}^2\right)}}\right) = Q\left(\sqrt{\mathrm{SNR}}\right), \tag{A.1}$$

where

$$\mathrm{SNR} = \frac{E_b}{2\left(N_0 + 2R_bE_b\sum_{k=2}^{N_u}\int_0^{T_M}\left(R_{n,l}^{(k)}(\tau)\right)^2 d\tau\right)}, \tag{A.2}$$

and $R_b = 1/N_sT_f$ is the data rate and $E_b = N_sE_{rx}$ is the received energy at the receiver. Since each decision is independent, the average probability of bit error is

$$Pr_b = \frac{1}{N}\sum_{l=0}^{N-1} P_l, \tag{A.3}$$

where N is the total number of correlators for N-bit symbols transmission. The correct decision of the lth correlator is $1 - P_l$. The received symbol is perfect if all correlators make correct decisions. Since decisions are independent, the probability of correct decision for a symbol can be defined as

$$P_c = \prod_{l=0}^{N-1}(1 - P_l). \tag{A.4}$$

The probability of symbol error rate can be calculated by using (A.1). The probability of symbol error rate can be expressed as

$$P_r = (1 - P_c) = \left(1 - \prod_{l=0}^{N-1}(1 - P_l)\right) = \left(1 - \prod_{l=0}^{N-1}\left(1 - Q\left(\sqrt{\mathrm{SNR}}\right)\right)\right). \tag{A.5}$$

B. MULTIPATH ENVIRONMENTS

B.1. Interpulse interference

The term $\mathrm{IPI}_q^{(1)}$ of user 1 in the qth correlator can be expressed from (17) as

$$\begin{aligned}\mathrm{IPI}_q^{(1)} &= \sqrt{E_{tr}^{(1)}}\sum_{j=0}^{N_s-1}\sum_{p=1}^{L_p}\sum_{\substack{l=1\\ l\neq p}}^{L_p}\alpha_p^{(1)}\alpha_l^{(1)} \\ &\quad\times\int_0^{T_f}\left(w_q^{(1)}\left(t - c_j^{(1)}T_c - \tau_l^{(1)}\right)w_q^{(1)}\left(t - c_j^{(1)}T_c - \tau_p^{(1)}\right)\right)dt \\ &= \sqrt{E_{tr}^{(1)}}N_s\sum_{p=1}^{L_p}\sum_{\substack{l=1\\ l\neq p}}^{L_p}\alpha_p^{(1)}\alpha_l^{(1)}R_{qq}^{(1,1)}\left(\tau_l^{(1)} - \tau_p^{(1)}\right),\end{aligned} \tag{B.1}$$

where $R_{qq'}^{(k,k)}\left(\tau_l^{(1)} - \tau_p^{(1)}\right) = \int_0^{T_f} w_q^{(k)}(t)w_{q'}^{(k)}\left(t - \tau_l^{(1)} - \tau_p^{(1)}\right)dt$ and $q' \in \{0, 1, \ldots, N-1\}$. The corresponding average variance of

$\mathrm{IPI}_q^{(1)}$ for the N_sT_f time frames is σ_{IPI}^2 and can be expressed as

$$\begin{aligned}\sigma_{\mathrm{IPI}}^2 &= \frac{E\left\{\left(\mathrm{IPI}_q^{(1)}\right)^2\right\} - \left(E\left\{\mathrm{IPI}_q^{(1)}\right\}\right)^2}{N_sT_f} \\ &= E_{tr}^{(1)}N_sT_f^{-1}E\left\{\left(\sum_{\substack{p=1\\ l\neq p}}^{L_p}\sum_{l=1}^{L_p}\alpha_p^{(1)}\alpha_l^{(1)}\times R_{qq}^{(1,1)}\left(\tau_l^{(1)}-\tau_p^{(1)}\right)\right)^2\right\} \\ &= E_{tr}^{(1)}N_sT_f^{-1}\sum_{p=1}^{L_p}\sum_{l=1}^{L_p}\sum_{\substack{p'=1\\ p'\neq p}}^{L_p}\sum_{\substack{l'=1\\ l'\neq l}}^{L_p}\alpha_p^{(1)}\alpha_l^{(1)}\alpha_{p'}^{(1)}\alpha_{l'}^{(1)}X(\Delta),\end{aligned} \tag{B.2}$$

where $X(\Delta) = E\{R_{qq}^{(1,1)}(\tau_l^{(1)}-\tau_p^{(1)})R_{qq}^{(1,1)}(\tau_{l'}^{(1)}-\tau_{p'}^{(1)})\}$.

B.2. Multipulse interference

The term $\mathrm{MPI}_q^{(1)}$ of user 1 in the qth correlator can be written from (17) as

$$\begin{aligned}\mathrm{MPI}_q^{(1)} &= \sqrt{E_{tr}^{(1)}}\sum_{j=0}^{N_s-1}\sum_{p=1}^{L_p}\sum_{\substack{l=1\\ l\neq p}}^{L_p}\sum_{\substack{m=1\\ m\neq q}}^{N}\alpha_p^{(1)}\alpha_l^{(1)} \\ &\quad\times\int_0^{T_f}\left(w_q^{(1)}\left(t-c_j^{(1)}T_c-\tau_l^{(1)}\right)w_q^{(1)}\left(t-c_j^{(1)}T_c-\tau_p^{(1)}\right)\right)dt \\ &= \sqrt{E_{tr}^{(1)}}N_s\sum_{p=1}^{L_p}\sum_{\substack{l=1\\ l\neq p}}^{L_p}\sum_{\substack{m=1\\ m\neq q}}^{N}\alpha_p^{(1)}\alpha_l^{(1)}R_{qm}^{(1,1)}\left(\tau_l^{(1)}-\tau_p^{(1)}\right).\end{aligned} \tag{B.3}$$

The average variance of σ_{MPI}^2 can be expressed as similar way of (B.2)

$$\sigma_{\mathrm{MPI}}^2 = E_{tr}^{(1)}N_sT_f^{-1}\sum_{p=1}^{L_p}\sum_{l=1}^{L_p}\sum_{\substack{p'=1\\ p'\neq p}}^{L_p}\sum_{\substack{l'=1\\ l'\neq l}}^{L_p}\sum_{\substack{m=1\\ m\neq q}}^{N}\sum_{\substack{m'=1\\ m'\neq q'}}^{N}\alpha_p^{(1)}\alpha_l^{(1)}\alpha_{p'}^{(1)}\alpha_{l'}^{(1)}Y(\Delta), \tag{B.4}$$

where $Y(\Delta) = E\{R_{qm}^{(1,1)}(\tau_l^{(1)}-\tau_p^{(1)})R_{q'm'}^{(1,1)}(\tau_{l'}^{(1)}-\tau_{p'}^{(1)})\}$.

B.3. Multiaccess interference

The term $\mathrm{MAI}_q^{(1)}$ of OOK-PSM schemes for the N_u users can be written from (17) as

$$\begin{aligned}\mathrm{MAI}_q^{(1)} &= \sum_{k=2}^{N_u}\sqrt{E_{tr}^{(k)}}\sum_{j=0}^{N_s-1}\sum_{p=1}^{L_p}\sum_{l=1}^{L_p}\alpha_l^{(k)}\alpha_p^{(1)} \\ &\quad\times\int_0^{T_f}\left(w_q^{(k)}\left(t-c_j^{(k)}T_c-\tau_l^{(k)}\right)w_{q'}^{(1)}\left(t-c_j^{(1)}T_c-\tau_p^{(1)}\right)\right)dt \\ &= N_s\sum_{k=2}^{N_u}\sqrt{E_{tr}^{(k)}}\sum_{p=1}^{L_p}\sum_{l=1}^{L_p}\alpha_l^{(k)}\alpha_p^{(1)}R_{qq'}^{(1,k)}(\Delta'),\end{aligned} \tag{B.5}$$

where $\Delta_1 = (c_j^{(1)}-c_j^{(k)})T_c - (\tau_p^{(1)}-\tau_l^{(k)})$.

The variance of σ_{MAI}^2 over the N_sT_f time frames can be expressed as similar way of (B.2)

$$\begin{aligned}\sigma_{\mathrm{MAI}}^2 &= N_sT_f^{-1}\sum_{k=2}^{N_u}\sum_{k'=2}^{N_u}\sqrt{E_{tr}^{(k)}}\sqrt{E_{tr}^{(k')}} \\ &\quad\times\sum_{p=1}^{L_p}\sum_{l=1}^{L_p}\sum_{p'=1}^{L_p}\sum_{l'=1}^{L_p}\alpha_p^{(1)}\alpha_l^{(k)}\alpha_{p'}^{(1)}\alpha_{l'}^{(k')}V(\Delta'),\end{aligned} \tag{B.6}$$

where $V(\Delta') = E\{R_{qq'}^{(1,k)}(\Delta_1)R_{qq'}^{(1,k')}(\Delta_2)\}$, and $\Delta_2 = (c_j^{(1)}-c_j^{(k')})T_c - (\tau_{p'}^{(1)}-\tau_{l'}^{(k')})$.

B.4. AWGN noise in multipath

$N_q^{(1)}$ is the AWGN generated by qth correlator and can be expressed from (17) as

$$N_q^{(1)} = \sum_{j=0}^{N_s-1}\sum_{p=1}^{L_p}\alpha_p^{(1)}\int_0^{T_f}n(t)w_q^{(1)}\left(t-c_j^{(1)}T_c-\tau_p^{(1)}\right)dt. \tag{B.7}$$

The corresponding noise is

$$\begin{aligned}\sigma_N^2 &= \frac{E\left\{\left(N_q^{(1)}\right)^2\right\} - \left(E\left\{N_q^{(1)}\right\}\right)^2}{N_sT_f} \\ &= N_s\left(\sum_{p=1}^{L_p}\alpha_p^{(1)}\right)^2E\left\{\int_0^{T_f}n(t)n(t)dt\right\} \\ &= \frac{N_0N_s\left(\sum_{p=1}^{L_p}\alpha_p^{(1)}\right)^2}{2}.\end{aligned} \tag{B.8}$$

REFERENCES

[1] S. Majhi, A. S. Madhukumar, and A. B. Premkumar, "Reduction of UWB interference at NB systems based on a generalized pulse waveform," *IEICE Electronics Express*, vol. 3, no. 14, pp. 361–367, 2006.

[2] G. Durisi, J. Romme, and S. Benedetto, "A general method for SER computation of M-PAM and M-PPM UWB systems for indoor multiuser communications," in *Proceedings of IEEE Global Telecommunications Conference (GLOBECOM '03)*, vol. 2, pp. 734–738, San Francisco, Calif, USA, December 2003.

[3] L. Bin, E. Gunawan, and L. C. Look, "On the BER performance of TH-PPM UWB using Parr's monocycle in the AWGN channel," in *Proceedings of IEEE Conference on Ultra Wideband Systems and Technologies*, pp. 403–407, Reston, Va, USA, November 2003.

[4] J. Foerster, "UWB channel modeling sub-committee report final," IEEEP802.15 Working Group for Wireless Personal Area Networks (WPANs), February 2003.

[5] M. Z. Win and R. A. Scholtz, "On the energy capture of ultrawide bandwidth signals in dense multipath environments," *IEEE Communications Letters*, vol. 2, no. 9, pp. 245–247, 1998.

[6] I. Guvenc and H. Arslan, "On the modulation options for UWB systems," in *Proceedings of IEEE Military Communications Conference (MILCOM '03)*, vol. 2, pp. 892–897, Monterey, Calif, USA, October 2003.

[7] M. Ghavami, L. B. Michael, S. Haruyama, and R. Kohno, "A novel UWB pulse shape modulation system," *Wireless Personal Communications*, vol. 23, no. 1, pp. 105–120, 2002.

[8] G. T. F. de Abreu, C. J. Mitchell, and R. Kohno, "On the design of orthogonal pulse-shape modulation for UWB systems using Hermite pulses," *Journal of Communications and Networks*, vol. 5, no. 4, pp. 328–343, 2003.

[9] X. Chu and R. D. Murch, "Multidimensional modulation for ultra-wideband multiple-access impulse radio in wireless multipath channels," *IEEE Transactions on Wireless Communications*, vol. 4, no. 5, pp. 2373–2386, 2005.

[10] S. Gezici, Z. Sahinoglu, H. Kobayashi, and H. V. Poor, "Ultra-wideband impulse radio systems with multiple pulse types," *IEEE Journal on Selected Areas in Communications*, vol. 24, no. 4, pp. 892–898, 2006.

[11] K. Usuda, H. Zhang, and M. Nakagawa, "M-ary pulse shape modulation for PSWF-based UWB systems in multipath fading environment," in *Proceedings of IEEE Global Telecommunications Conference (GLOBECOM '04)*, vol. 6, pp. 3498–3504, Dallas, Tex, USA, November-December 2004.

[12] C. J. Mitchell, G. T. F. de Abreu, and R. Kohno, "Combined pulse shape and pulse position modulation for high data rate transmissions in ultra-wideband communications," *International Journal of Wireless Information Networks*, vol. 10, no. 4, pp. 167–178, 2003.

[13] W. Hu and G. Zheng, "Orthogonal Hermite pulses used for UWB M-ary communication," in *Proceedings of the International Conference on Information Technology: Coding and Computing (ITCC '05)*, vol. 1, pp. 97–101, Las Vegas, Nev, USA, April 2005.

[14] S. Majhi, A. S. Madhukumar, and A. B. Premkumar, "Performance of orthogonal based modulation schemes for TH-UWB communication systems," *IEICE Electronics Express*, vol. 4, no. 8, pp. 238–244, 2007.

[15] F. Nekoogar, *Ultra-Wideband Communication*, Prentice Hall, Upper Saddle River, NJ, USA, 2005.

[16] S. Majhi, A. S. Madhukumar, A. B. Premkumar, and F. Chin, "M-ary signaling for ultra wideband communication systems based on pulse position and orthogonal pulse shape modulation," in *Proccedings of IEEE Wireless Communications and Networking Conference (WCNC '07)*, pp. 2795–2799, Kowloon, Hong Kong, March 2007.

[17] K. Siwiak and D. McKeown, *Ultra-Wideband Radio Technology*, John Wiley & Sons, New York, NY, USA, 2004.

[18] A. S. Madhukumar, Z. Ye, and S. Majhi, "Coexisting narrowband and ultra wideband systems: analysis of power spectral density and in-band interference power," *WSEAS Transactions on Communications*, vol. 6, no. 2, pp. 318–324, 2007.

[19] M. Z. Win, "Spectral density of random time-hopping spread-spectrum UWB signals with uniform timing jitter," in *Proceedings of IEEE Military Communications Conference (MILCOM '99)*, vol. 2, pp. 1196–1200, Atlantic City, NJ, USA, October-November 1999.

[20] I. Guvenc and H. Arslan, "Performance evaluation of UWB systems in the presence of timing jitter," in *Proceedings of IEEE Conference on Ultra Wideband Systems and Technologies*, pp. 136–141, Reston, Va, USA, Novemebr 2003.

[21] B. Hu and N. C. Beaulieu, "Precise bit error rate of TH-PPM UWB systems in the presence of multiple access interference," in *Proceedings of IEEE Conference on Ultra Wideband Systems and Technologies*, pp. 106–110, Reston, Va, USA, November 2003.

[22] T. Jia and D. I. Kim, "Analysis of average signal-to-interference-noise ratio for indoor UWB rake receiving system," in *Proceedings of the 61st IEEE Vehicular Technology Conference (VTC '05)*, vol. 2, pp. 1396–1400, Stockholm, Sweden, May-June 2005.

[23] L. Jiang, Y. Wang, and J. Guo, "The capacity of M-ary PPM ultra-wideband communication over multipath channels," in *Proceedings of IEEE International Symposium on Microwave, Antenna, Propagation and EMC Technology for Wireless Communication (MAPE '05)*, vol. 2, pp. 1606–1609, Beijing, China, August 2005.

[24] M. G. D. Benedetto and G. Giancola, *Understanding Ultra Wideband Radio Fundamentals*, Prentice Hall, Upper Saddle River, NJ, USA, 2004.

[25] K.-H. Kim, S. Choi, Y. Park, et al., "Enhanced noncoherent OOK UWB PHY and MAC for positioning and ranging," IEEE P802.15 Working Group for Wireless Personal Area Networks (WPANs), January 2005.

[26] T. Matsumoto, H. Ochiai, and R. Kohno, "Super-orthogonal convolutional coding with orthogonal pulse waveform for ultra wideband communications," in *Proceedings of the International Workshop on Ultra Wideband Systems; Joint with Conference on Ultra Wideband Systems and Technologies*, pp. 202–206, Kyoto, Japan, May 2004.

[27] K. Eshima, Y. Hase, S. Oomori, F. Takahashi, and R. Kohno, "M-ary UWB system using Walsh codes," in *Proceedings of IEEE Conference on Ultra Wideband Systems and Technologies (UWBST '02)*, pp. 37–40, Baltimore, Md, USA, May 2002.